Pathways toward Electric Field Induced Alignment of Block Copolymers

Thomas Thurn-Albrecht

Albert-Ludwigs-Universität, 79104 Freiburg, Germany

Jason DeRouchey and Thomas P. Russell*

Department of Polymer Science and Engineering, University of Massachusetts, Amherst, Massachusetts 01003

Rainer Kolb

ExxonMobil Research and Engineering Company, Annandale, New Jersey 08801

Received April 9, 2002

ABSTRACT: Using in situ small-angle X-ray scattering, the electric field induced orientation in a block copolymer having a cylindrical microdomain morphology was investigated. Studies were performed with the copolymer in different initial states. Beginning with a disordered copolymer, composition fluctuations are oriented by the electric field. Following cooling across the disorder-to-order-transition, microdomains are oriented parallel to the applied field. Beginning with a microphase-separated copolymer where the microdomains are oriented normal to the field, the domain orientation becomes unstable at high field strengths, and the microdomains reorient in a piecewise manner.

Introduction

Soft structures in ordered liquidlike materials can be oriented by relatively weak external forces, for example, in liquid crystalline materials. Recently, there has been an increasing interest in achieving similar control over the arrangement of the nanoscopic structures produced by the self-assembly of block copolymers in thin films.[1,2] While shear is quite effective in orienting block copolymer microdomains in the bulk,[3] electric fields and interfacial interactions have been used to great advantage in thin films[4] to direct the self-assembly of ordered nanostructures.[5,6] Both lead to an orientation-dependent free energy and a corresponding equilibrium orientation of the microphase-separated structure.[4,7−11]

The driving force for electric field induced alignment is the orientation-dependent polarization in a material having domains that are anisotropic in shape. In situ studies that follow the pathway to electric field induced orientation in block copolymers are scarce, though a mechanism of alignment has been suggested on the basis of indirect evidence.[7,8,12] Beginning with a disordered or poorly ordered microphase-separated structure, Amundson suggested that the final oriented morphology is attained by a simultaneous orientation and ordering of the microdomains. Nuclei, initially oriented at random, are thought to be rotated by the electric field during growth.[7] With such a process, the degree of orientation achieved would depend critically on the stage in the growth process when orientation occurred. However, the order-to-disorder transition in block copolymers, although first order, is accompanied by strong composition fluctuations in the disordered state that may be influenced by the applied field.

Here, experiments on the development of order and orientation in a block copolymer with cylindrical microdomains are reported. In situ small-angle X-ray scattering studies were performed as the copolymer was cooled from the disordered state into the ordered state under the influence of a strong electric field. The electric field was found to orient composition fluctuations in the disordered state, leading to a preferred growth of well-aligned nuclei. This is contrasted with the case where ordered copolymer microdomains are initially misaligned with the applied field and a reorganization of microdomains must occur to achieve the final aligned morphology.

Experimental Section

Samples. Asymmetric diblock copolymers of polystyrene and poly(methyl methacrylate) P(S-*b*-MMA) with a weight-average molecular weight of 3.9×10^4 and polydispersity of 1.08 with a PMMA volume fraction of 0.29 were synthesized anionically. As shown previously, the copolymer microphase separates into cylindrical microdomains arranged on a hexagonal lattice with a periodicity of 23.3 nm at room temperature.[4] The order-to-disorder transition temperature of this copolymer was found to be 196 ± 2 °C as determined by optical microscopy. Films with a thickness of 20−30 μm were roll-pressed in the melt with a calendar and annealed at 170 °C between two 12.7 μm Kapton sheets that were coated on one side with 100 nm of Al, which served as electrodes. The thickness of the sample was controlled with Kapton spacers. To avoid electric shorting, one of the Al electrodes was placed in direct contact with the polymer, while the second was inverted with the Kapton in contact with the copolymer.

Small-Angle X-ray Scattering. Small-angle X-ray scattering experiments were performed on beamline X10A at the National Synchrotron Light Source (NSLS) at the Brookhaven National Laboratory. The X-ray beam was monochromated with a double bounce germanium monochromator ($\lambda = 1.5$ Å); the size of the beam on the sample was ∼0.7 mm (horizontal) × 1.0 mm (vertical). The detector, a Bruker CCD camera, was set at a distance of ∼2.2 m from the sample. A helium-filled tube between the sample and the detector was used to eliminate air scattering. The sample was placed in a temperature-controlled sample holder consisting of two metal plates with a horizontal slit-shaped opening (2 mm × 15 mm) that allowed the angle of incidence to be varied from 0° to 60° (0° was taken as normal incidence). Typical exposure times were 10 s.

Results

Cylinders oriented perpendicular to a plane give rise to a distinct scattering pattern. Figure 1 shows a

10.1021/ma020567v CCC: $22.00
Published on Web 09/04/2002

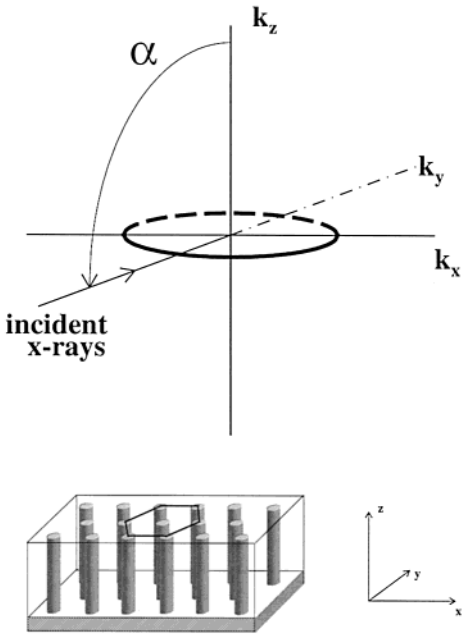

Figure 1. Intensity distribution of the (01) reflection in reciprocal space for a hexagonal array of cylinders standing perpendicular to the surface of the film. A schematic of one grain of the cylinders is shown in the lower portion. In an actual sample, the grains are arranged randomly within the plane giving rise to a ring of diffraction in the k_x-k_y plane. The incident X-ray angle, α, is changed by a rotation of the sample about the k_x axis. The diagrams shown corresponds to $\alpha = 90°$.

schematic diagram of the distribution of the dominant (10) reflection in reciprocal space for a random orientation of grains of hexagonally packed cylinders oriented normal to the surface of a film ($x-y$ plane). A schematic of one such grain is also shown. The lattice constant is $a = 4\pi/\sqrt{3}q_{10}$, where q_{10} is the scattering vector, q, corresponding to the maximum in the scattering and $q = (4\pi/\lambda)\sin\theta$ where 2θ is the scattering angle. With no preferred orientation of the grains in the plane of the film, the intensity is distributed equally along a ring in the k_x-k_y plane. Visible in the experiment is the intersection of this ring with the Ewald sphere, which, for small-angle scattering, can be approximated by a plane normal to the incident beam. For normal incidence ($\alpha = 0°$), the scattering pattern consists of a ring; for all other angles, two arcs or spots on the axis of rotation (here the horizontal axis) are seen. For an isotropic sample, the scattering pattern consists of a homogeneous ring independent of the incidence angle α.

The development of order and orientation was examined as the copolymer was cooled from the disordered into the ordered state under an applied external electric field. All measurements were taken with $\alpha = 45°$. A typical scattering pattern is shown in Figure 2A. The arcs on the left- and right-hand side of the pattern indicate alignment of the cylindrical microdomains parallel to the electric field (perpendicular to the plane of the sample). In Figure 2B, the intensity, integrated in q over the peak, is given as a function of the azimuthal angle Ω. Prior to the experiment, the sample was heated to $T = 205$ °C, i.e., into the disordered state (curve 1). An electric field of 30 V/μm was then applied, producing the results in curves 2 and 3 measured several minutes later. This field strength is well above the critical field strength where orientation of the

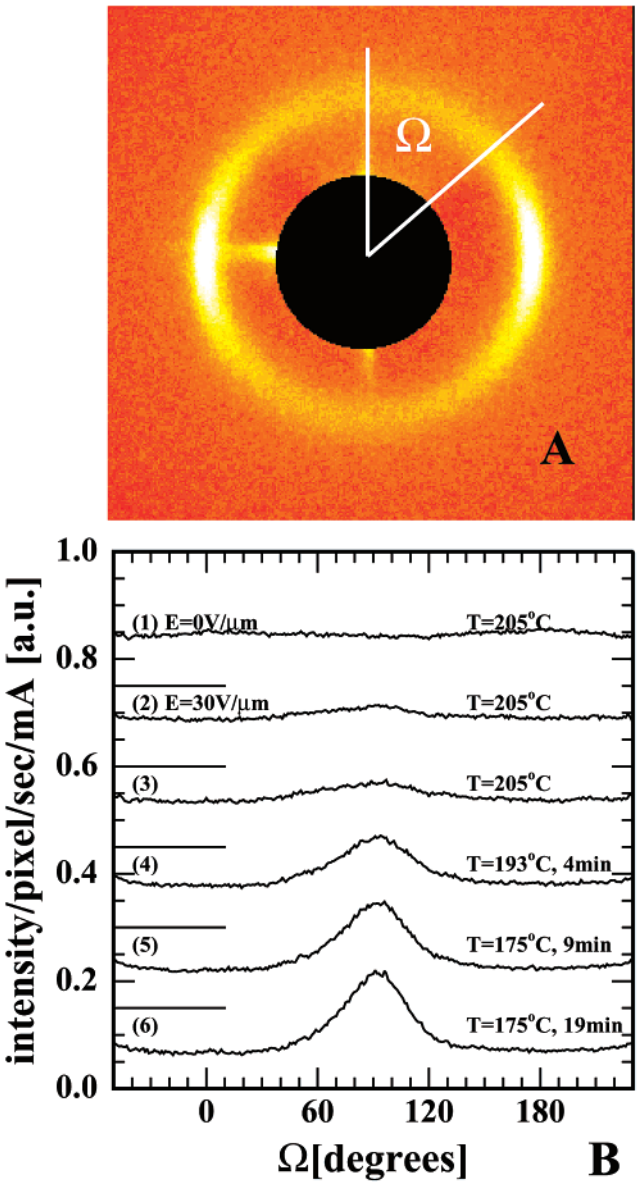

Figure 2. Series of SAXS measurements following the process of orientation and ordering in an electric field. (A) Exemplary scattering pattern corresponding to data set (4) below. All measurements were taken with an angle of incidence $\alpha = 45°$. (B) Scattering intensity as shown in (A) integrated in q over the range of the peak as a function of azimuthal angle Ω (the left part of the image is excluded). Data sets (1−3) were measured in the disordered phase without (1) and with (2, 3) electric field ($E = 30$ V/μm). Subsequent cooling below the order-to-disorder transition temperature induces growth of an ordered, oriented microphase structure (4−6). The time is quench time at the ordering temperature. Consecutive measurements are shifted relative to each other; the respective zero positions are indicated.

microdomains occurs.[4] The sample was then cooled to 175 °C (curves 5 and 6), which is below the disorder-to-order transition temperature, and formation of the microphase-separated morphology was followed in real time by SAXS. The onset of order upon cooling can be directly identified by the decrease in the width and increase in intensity of the peak as shown in parts A and B of Figure 3, respectively. The scattered intensity as a function of q around the first reflection and the fwhm of this reflection as a function of time are shown. The scattering pattern of the disordered melt without an applied field consists of a broad isotropic ring arising

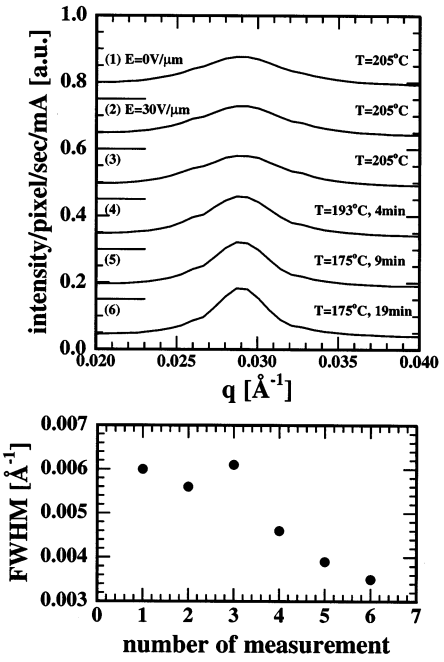

Figure 3. (A) Integrated intensity vs scattering vector q and (B) fwhm of the peak as a function of time, determined from the scattering profiles in Figure 2. The first three measurements were taken in the disordered phase; subsequently, the sample was cooled to the ordered state.

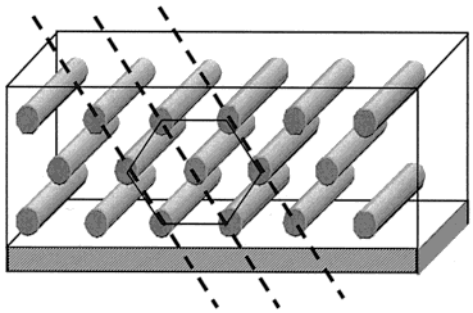

Figure 4. Schematic of the cylindrical phase of a block copolymer with the cylinders oriented parallel to the substrate. The lattice planes corresponding to the reflection used for the measurement shown in Figure 5 are indicated by a broken line.

from composition fluctuations. The scattering pattern becomes anisotropic with the application of the electric field. Fluctuations parallel to the electric field are enhanced, while fluctuations perpendicular to the field are suppressed. Consecutive measurements (curves 2 and 3) show that this is a stationary, equilibrium state. Upon cooling below the order−disorder transition temperature, only the equatorial intensity of the peak increases (around $\Omega = 90°$ and $\Omega = 270°$). This indicates that there is a strong orientation of the microdomains from the very onset of ordering. The microphase-separated structure grows directly along the preferred direction established by anisotropic composition fluctuations.

In the absence of an applied field, preferential interactions of one block with the electrode interfaces forces an alignment of the cylindrical microdomains parallel to the plane of the film, as shown schematically in Figure 4. Using the sample preparation conditions described above, large grains of ordered cylindrical microdomains oriented parallel to the surface were found, and a section of the sample was chosen where

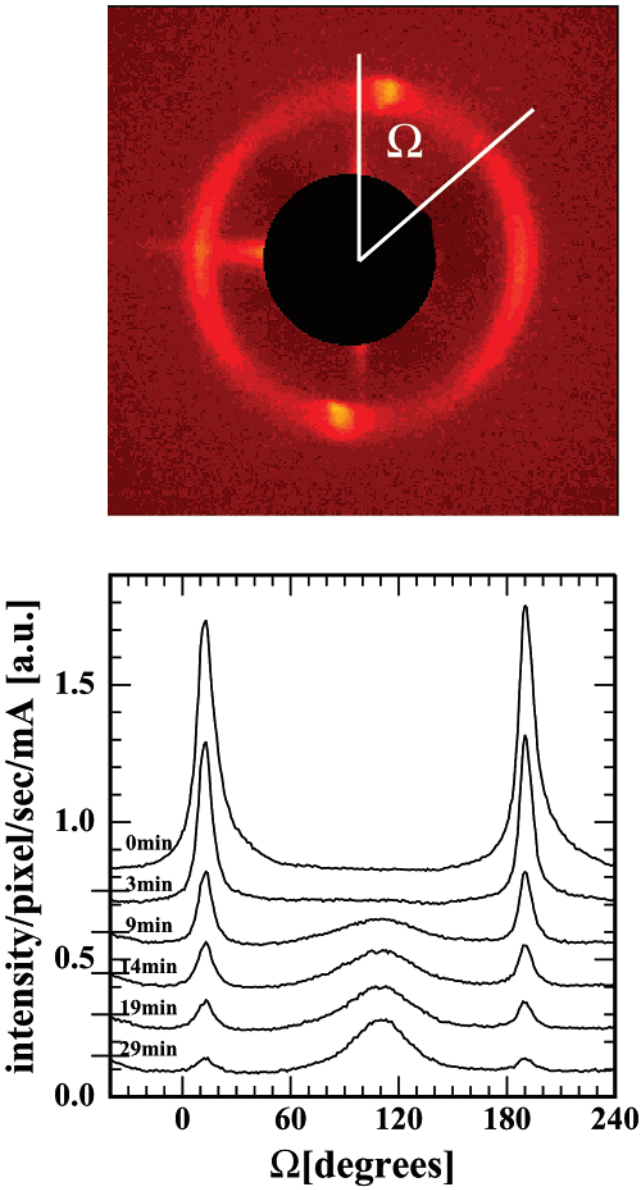

Figure 5. Series of SAXS measurements following electric field induced reorientation ($E = 30$ V/μm) of the microphase structure starting from a sample with the cylinders aligned parallel to the substrate. Measurements were taken at a temperature of 185 °C and an angle of incidence $\alpha = 30°$. (A) A typical scattering pattern (corresponding to data set marked 9 min below). The reflections on top and bottom are caused by parts of the sample aligned parallel to the substrate. Scattering on the left and right corresponds to parts of the sample aligned perpendicular to the substrate. (B) Scattering intensity as shown in (A) integrated in q over the range of the peak as a function of azimuthal angle Ω. The time elapsed since the field was applied is indicated on the right-hand side of the curves.

the scattering volume consisted of one dominant grain. The sample was rotated in the beam so that a pair of first-order Bragg reflections were observable. This corresponded to an angle of incidence of ∼30°. A typical scattering profile is shown in Figure 5 that captures the intermediate stage of reorientation. Two sharp spots around $\Omega = 0°$ and 180° are seen, which arise from microdomains oriented parallel to the film surface. The diffuse arcs on the equator indicate that some of the cylinders were aligned normal to the surface. The scattering intensity as a function of the azimuthal angle is shown in the lower part of Figure 5. The data show

that a reorientation of the original structure takes place. A decrease in intensity of the original two reflections is accompanied by an increase in intensity around $\Omega = 90°$ and 270°. This can be attributed to cylinders aligned normal to the surface by the electric field. The intensity visible in the final state is lower than the intensity of the original reflections since there are many grains of cylinders oriented normal to the film surface but with different orientations of the hexagonal lattice within the plane. Only some of these grains contribute to the scattering intensity at a fixed position of the sample.

Discussion

Electric field induced alignment of block copolymer microdomains was previously discussed in terms of the rotation of grains and the movement of grain boundaries under the influence of the electric field.[7,9,12] These experiments were done with electric fields about an order of magnitude lower than those used here. In the studies reported here, the results in Figures 2 and 5 clearly show that the alignment of the microdomains can be achieved from different initial states following different pathways. From the disordered state, the orientation of concentration fluctuations leads to the formation of oriented nuclei and, subsequently, oriented microdomains. An intermediate state where grains were too small to be oriented was not detected. The amplitude of the orientation-dependent electrostatic energy per unit volume of a composition fluctuation of amplitude A in an electric field E_0 is given by[7]

$$\Delta E = \frac{1}{2}\epsilon_0\epsilon_D E_0^2\left(\frac{\beta}{\epsilon_D}\right)^2 A^2$$

Here[7] $\beta = d\epsilon/d\varphi$ with φ being the local volume fraction of one of the copolymer components, ϵ_D is the dielectric constant in the absence of any composition fluctuations, and ϵ_0 is the permittivity in a vacuum. Amundson et al. estimated the minimal size l of a nucleus, where the orientation-dependent dielectric energy contribution becomes comparable to thermal energies kT. For an electric field of 1.8 V/μm, $l \approx 150$ nm. Since l scales as $E^{-2/3}$, one would expect l to be ~23 nm in an electric field of 30 V/μm. This is considerably less than l_c, the correlation length of composition fluctuations in the disordered state, as estimated from the full width at half-maximum (fwhm), Δq, of the peak in the scattering intensity. From the data in Figure 3, l_c at 205 °C is ~100 nm (curve 2). Consequently, the observed orientation, even in the disordered state, is consistent with existing theoretical estimates. A crossover to the case considered by Amundson would be expected at $E \sim 3.3$ V/μm.

Let us turn now to the orientation of microphase-separated copolymers where the cylinders are oriented, initially, normal to the applied field. Here, a simple rotation of the original structure cannot occur. To enable reorientation via rotation of grains and/or a defect-mediated mechanism, the microdomains must become unstable, leading to a disruption of the grains into smaller pieces that are able to rotate and/or rearrange. Rather, the microdomains must be broken into smaller pieces that can rotate in the field. The results shown in Figure 5 indicates that this process does indeed take place. The reduction in the intensity of the meridonal reflections occurs with the simultaneous growth in the intensity of the reflection at 90°. Consequently, a piecewise orientation of grains of the cylindrical microdomains occurs to produce the final highly oriented microdomains.

Conclusion

Using in situ small-angle X-ray scattering, the orientation of an asymmetric diblock copolymer in a strong electric field was investigated. From the disordered melt, the applied field oriented concentration fluctuations that serve to template the formation of an oriented microphase-separated morphology. This might be of practical relevance for obtaining oriented materials with a high degree of perfection. It is reasonable to assume that the orientation of copolymers having a kinetically trapped, poorly ordered morphology, as obtained after spin-coating would occur by a similar route. However, for a copolymer having ordered microdomains, the data indicate that the applied field leads to an instability that enables the large grains in the initial copolymer to be broken up into smaller sections by the amplification of interfacial fluctuations similar to that observed on liquid surfaces and liquid bilayers exposed to electric fields.[14,15] Such a mechanism has also been postulated theoretically by Onuki and Fukuda and, more recently, by Tsori and Andelmann.[16,17] The exact lateral length scale of this instability remains a question for further investigation.

Acknowledgment. We are grateful to C. Stafford for the synthesis of the copolymers and to S. Bennett for technical support during the experiments at the NSLS. We thank the Sheldahl Company for supplying the aluminized Kapton. T.T.-A. acknowledges the support of the Deutsche Forschungsgemeinschaft. This work was also supported by the Department of Energy's Office of Basic Energy Science and the National Science Foundation-supported Materials Research Science and Engineering Center. Experiments were carried out at the National Synchrotron Light Source, Brookhaven National Laboratory, which is supported by the U.S. Department of Energy, Division of Materials Sciences and Division of Chemical Sciences.

References and Notes

(1) Russell, T. P. *Curr. Opin. Colloid Interface Sci.* **1996**, *1*, 107.
(2) Matsen, M. W. *Curr. Opin. Colloid Interface Sci.* **1998**, *3*, 1998.
(3) Hamley, I. W. *The Physics of Block Copolymers*; Oxford University Press: Oxford, 1998.
(4) Thurn-Albrecht, T.; DeRouchey, J.; Russell, T. P.; Jaeger, H. M. *Macromolecules* **2000**, *33*, 3250−3253.
(5) Thurn-Albrecht, T.; Steiner, R.; DeRouchey, J.; Stafford, C.; Huang, E.; Bal, M.; Tuominen, M.; Hawker, C. J.; Russell, T. P. *Adv. Mater.* **2000**, *12*, 787−791.
(6) Thurn-Albrecht, T.; Schotter, J.; Kästle, G. A.; Emley, N.; Shibauchi, T.; Krusin-Elbaum, L.; Guarini, K.; Black, C. T.; Tuominen, M. T.; Russell, T. P. *Science* **2000**, *290*, 2126−2129.
(7) Amundson, K.; Helfand, E.; Davis, D. D.; Quan, X.; Patel, S. S.; Smith, S. D. *Macromolecules* **1991**, *24*, 6546.
(8) Amundson, K.; Helfand, E.; Quan, X.; Smith, S. D. *Macromolecules* **1993,** *26*, 2698.
(9) Amundson, K.; Helfand, E.; Quan, X.; Hudson, S. D.; Smith, S. D. *Macromolecules* **1994**, *27*, 6559.
(10) Boker, A.; Knoll, A.; Elbs, H.; Abetz, V.; Muller, A. H. E.; Krausch, G. *Macromolecules* **2002**, *35*, 1319.
(11) Mansky, P.; DeRouchey, J.; Mays, J.; Cook, D. C.; Morkved, T.; Jaeger, H.; Russell, T. P. *Macromolecules* **1998**, *31*, 4399.
(12) Morkved, T.; Lu, M.; Urbas, A. M.; Ehrichs, E. E.; Jaeger, H. M.; Mansky, P.; Russell, T. P. *Science* **1996**, *273*, 931.
(13) DeRouchey, J.; Thurn-Albrecht, T.; Russell, T. P. Manuscript in preparation.

(14) Schäffer, E.; Thurn-Albrecht, T.; Russell, T. P.; Steiner, U. *Nature (London)* **2000**, *403*, 874.
(15) Schäffer, E.; Thurn-Albrecht, T.; Russell, T. P.; Steiner, U. *Europhys. Lett.* **2001**, *53*, 518.
(16) Onuki, A.; Fukuda, J. *Macromolecules* **1995**, *28*, 8788.
(17) Tsori, Y.; Andelmann, D. *Macromolecules* **2002**, *35*, 5161.

MA020567V